RAA 2016 Vol. **16** No. **3**, 37 (10pp) doi: 10.1088/1674–4527/16/3/037
http://www.raa-journal.org *http://iopscience.iop.org/raa*

Research in Astronomy and Astrophysics

GalevNB: a conversion from N-body simulations to observations

Xiao-Ying Pang[1,2,5], Christoph Olczak[1,3], Di-Feng Guo[1,3], Rainer Spurzem[1,4,3,6] and Ralf Kotulla[7]

[1] National Astronomical Observatories and Key Laboratory of Computational Astrophysics, Chinese Academy of Sciences, Beijing 100012, China; *xypang@bao.ac.cn*
[2] Shanghai Institute of Technology, Shanghai 201418, China
[3] Astronomisches Rechen-Institut, Zentrum für Astronomie der Universität Heidelberg, Mönchhofstr. 12–14, 69120 Heidelberg, Germany
[4] Kavli Institute for Astronomy and Astrophysics, Peking University, Beijing 100871, China
[5] Key Lab for Astrophysics, Shanghai Normal University, Shanghai 200234, China
[6] Key Laboratory of Frontiers in Theoretical Physics, Institute of Theoretical Physics, Chinese Academy of Sciences, Beijing 100190, China
[7] Department of Astronomy, University of Wisconsin - Madison, 475 N Charter St, Madison WI 53706, USA

Received 2015 January 6; accepted 2015 September 17

Abstract We present `GalevNB` (`Galev` for N-body simulations), a utility that converts fundamental stellar properties of N-body simulations into observational properties using the `GALEV` (GAlaxy EVolutionary synthesis models) package, and allowing direct comparisons between observations and N-body simulations. It works by converting fundamental stellar properties, such as stellar mass, temperature, luminosity and metallicity into observational magnitudes for a variety of filters used by mainstream instruments/telescopes, such as HST, ESO, SDSS, 2MASS, etc., and into spectra that span the range from far-UV (90 Å) to near-IR (160 μm). As an application, we use `GalevNB` to investigate the secular evolution of the spectral energy distribution (SED) and color magnitude diagram (CMD) of a simulated star cluster over a few hundred million years. With the results given by `GalevNB` we discover a UV-excess in the SED of the cluster over the whole simulation time. We also identify four candidates that contribute to the FUV peak: core helium burning stars, second asymptotic giant branch (AGB) stars, white dwarfs and naked helium stars.

Key words: stars: kinematics and dynamics — stars: C-M diagrams — stars: AGB and post-AGB — stars: white dwarf

1 INTRODUCTION

Models of dense stellar systems, such as globular or young dense stellar clusters, or nuclear star clusters with or without a massive central black hole, require direct N-body simulations, which at least resolve and follow all stellar orbits in a star cluster as precisely as possible given the usable hardware and computing time. But due to the strong dependence on initial conditions of the gravitational N-body problem, which originates from close encounters, the system is physically and numerically unstable (Miller 1966). Therefore results of direct high-accuracy N-body simulations should always be carefully analyzed, as they represent individual realizations of physically possible solutions. In other words, small variations of initial conditions may lead to different results with regard to individual objects or events. Nevertheless, the coarse-grained evolution (densities, distribution functions) is quite good at following expectations from statistical mechanics (see e.g. Giersz & Spurzem 1994; Spurzem & Aarseth 1996). These simulations are an excellent tool to examine and study physical processes in star clusters.

The series of high-accuracy direct N-body codes developed by Sverre Aarseth (Aarseth 1999, 2003) is among the most widely used if not *the* most widely used code in this field. Its most notable features are the fourth-order Hermite integration scheme, the hierarchically blocked individual time steps (Makino & Aarseth 1992), the Kustaanheimo-Stiefel (KS) regularization for strong interactions (Kustaanheimo & Stiefel 1965) and its generalizations for few-body subsystems (chain regularization, Mikkola & Aarseth 1993), and the Ahmad-Cohen neighbor scheme (Ahmad & Cohen 1973). `NBODY6++` is the current massively parallel version of `NBODY6` (Spurzem 1999; Spurzem et al. 2008), and `NBODY6++GPU` adds to it the use of accelerated many-core hardware (incorporating graphics processing units (GPUs)) on every node (Wang et al. 2015).

In Wang et al. (2015), it becomes clear that direct N-body simulations with a million particles are feasible now. The challenges associated with the resulting massive amount of simulated data and possible approaches to their management are addressed in Wang et al. (2015).

However, the output parameters of N-body simulations are mostly theoretical values. To make a direct comparison between our simulation data and observations, we combine `GALEV` (GALaxy EVolutionary synthesis models; Kotulla et al. 2009), a flexible algorithm to combine astrophysical colors in many filters and spectra of stars (Lejeune et al. 1997, 1998) or sets of stars, with `NBODY6++GPU` simulations.

In this paper, we present this new code: `GalevNB` (`Galev` for N-body simulation) and its application in `NBODY6++GPU` simulation data. By adapting subroutines from `GALEV`, `GalevNB` can produce spectra that span the range from far-UV (FUV) at 90 Å to far IR at 160 μm, with a spectral resolution of 20 Å in the UV-optical and 50–100 Å in the near IR. Given a list of requested filters in the Hubble Space Telescope (HST), ESO, SDSS, 2MASS, etc., `GalevNB` convolves the spectra with the filter response functions and applies the chosen zero-points (Vegamag, ABmag and STmag) to yield absolute magnitudes. `GalevNB` bridges theoretical parameters and their observed values, thus allowing us to understand the color and spectral evolution of star clusters, and to determine the initial conditions and parameters of star cluster simulations with a direct comparison to observations.

Though most Galactic and many Local Group clusters are resolved, observing individual stars in extragalactic star clusters is extremely challenging due to severe crowding. Therefore, integrated photometry and spectroscopy have been used to identify extragalactic star clusters and obtain parameters (Bica et al. 1996a; Sarajedini et al. 2007; Peng et al. 2008, 2009; Johnson et al. 2012), and even to investigate multiple stellar populations (Peacock et al. 2013). Using the imaging obtained with the High Resolution Channel of the Advanced Camera for Surveys on board HST, Larsen et al. (2011) manage to construct color magnitude diagrams (CMDs) for several extragalactic star clusters within 5 Mpc. However, for the very distant star clusters, such as the ones in the Antennae Galaxies ($\sim 22\,\mathrm{Mpc}$, Whitmore et al. 2007; Bastian et al. 2009), or in the Virgo cluster ($\sim\ 16.5\,\mathrm{Mpc}$, Peng et al. 2008, 2009), studies of individual stars are still not possible. Integrated colors can generally be used to derive the age of star clusters (Elson & Fall 1985). However, metal variation, stochastic effects (Girardi et al. 1995), and dynamical evolution (Fleck et al. 2006) will change integrated colors. Therefore, integrated photometry may not be enough to decouple the stellar and dynamical effects of distant star clusters. With `GalevNB` producing observational magnitudes and spectra for N-body simulations, it allows us to investigate stellar evolution and dynamics (via colors and spectra) in distant star clusters at the same time, and even make predictions that can be verified with observations.

In this paper, we carry out star cluster simulations with `NBODY6++GPU` codes, and use `GalevNB` to produce observational data for the simulated cluster. The computational methods of `NBODY6++GPU` simulations are summarized in Section 2. An introduction to the structure and execution procedure of `GalevNB` is presented in Section 3. The observational features of the simulated cluster, CMDs and spectral energy distributions (SEDs) are outlined in Section 4. Finally, we present our discussion and summary in Section 5.

2 COMPUTATIONAL METHOD AND INITIAL CONDITIONS

The model clusters in this work are evolved using `NBODY6++GPU` which is the `MPI` parallel version based on the state-of-the-art direct N-body integrator `NBODY6GPU` (Aarseth 2003; Nitadori & Aarseth 2012). Gravitational forces are computed using a fourth-order Hermite integration scheme with block time steps (and without softening). The code includes algorithms for stellar and binary evolution (Tout et al. 1997; Hurley et al. 2000) and deals directly with perturbations to binary orbits, collisions and mergers, formation of three- and four-body subsystems, exchange interactions and tidal capture. The treatment of close encounters constitutes a large part of the code.

We set up a simple dynamical model of a massive stellar cluster as an example for `GalevNB` to work on. The stellar system is initially gas-free and is assumed to be in virial equilibrium as an approximation after losing gas (i.e. the ratio of kinetic to potential energy is $Q_{\rm vir} = 0.5$). The single-aged population is run with $N_0 = 10\,000$ single stars. Million-particle simulations of star clusters will be shown in our forthcoming paper. The IMF is set up according to Kroupa (2001) with fixed lower and upper mass limits, $m_{\rm l} = 0.1\,M_{\odot}$ and $m_{\rm u} = 20\,M_{\odot}$, respectively, resulting in an initial cluster mass of $M_0 = 4.7\times10^3\,M_{\odot}$. To simplify the computation, stars are distributed according to the Plummer model with a scale radius of 0.59 pc, which does not differ significantly from the King model with $W_0 = 6$, except in the outermost regions with low density. The models have an initial half-mass radius $R_{\rm hm} = 0.76$ pc, and are not primordially mass segregated. We set the metallicity to sub-solar metallicity $Z_{\odot} = 0.001$, which is similar to the halo population of Galactic globular clusters. Note that our simulated star cluster is still less massive than a typical Galactic globular cluster. But here we are interested in special spectral features, such as the production of UV-bright stars, and aim to relate the current simulations to future million particle simulations.

Since our primary interest is the short-term stellar evolution, we therefore carry out a simulation of 3000 N-body time units (corresponding to 655.6 Myr) with dynamical and internal stellar evolution. Snapshots of the simulation are selected to display in this paper to indicate the presence of UV-bright stars (see Sect. 4).

3 GALEVNB: GALEV FOR N-BODY SIMULATIONS

3.1 GalevNB Structure

In this section, we introduce the GalevNB structure and its parameters. The main program of GalevNB is GalevNB.f90, which parses single snapshot files (stellar evolution only) generated by NBODY6++GPU (NBODY6++)/ NBODY6GPU (NBODY6). It invokes seven subroutines (startomaginit, specint_initialize, reset_weights, startomag, add_star, spec2mag, spec_output) that are part of the GALEV package to convert effective temperature, stellar luminosity, metallicity and mass into observational magnitudes and spectra. The functions incorporated in these routines are presented in Table 1. The GalevNB package contains four folders: (1) spectral_templates, in which all the spectral template files from the BaSeL library of model atmospheres (Lejeune et al. 1997, 1998) are stored; (2) standard_filters, containing a large set of filter response functions (FUV, NUV, U, B, V, R, I, J, H, K) that are used as standard reference filters; (3) filter_response_curves, including filter response functions from magnitude systems of HST, ESO instruments, 2MASS, SDSS, Johnson, and Cousins in separate subfolders. We also provide a choice of user-specified filter response functions. Information about the entire set of available filters is presented in the file filterlist.dat. Please be aware that filterlist.dat, in which the users specify their own choice of magnitude system by uncommenting the row of a chosen filter, MUST be presented in the same directory as the NBODY6++GPU (NBODY6++)/ NBODY6GPU (NBODY6) snapshot files. The contents of the file, filterlist.dat, are presented in Table 2.

3.2 Installation and Usage of GalevNB

To compile GalevNB, the user should have C++ and Fortran installed. The input file of GalevNB should be a single snapshot output from NBODY6++GPU (NBODY6++)/ NBODY6GPU (NBODY6) simulations. In case of a file containing all snapshots (called sev.83 in NBODY6++GPU / NBODY6++ and fort.83 in NBODY6GPU / NBODY6), we provide the user with a shell script generate_snapshots.sh in the folder scripts for retrieving single snapshot data out of sev.83 and fort.83. The user can select his/her preferred filters (maximum 20) by uncommenting the row of the corresponding filter in filterlist.dat, and choose his/her desired magnitude system (Table 2). Magnitudes of individual stars and the whole cluster, and spectra of the cluster or chosen stellar types are produced, separately. The code for GalevNB is published online[1]. Users can download it through the internet. We also provide examples of output files from NBODY6++GPU and GalevNB on the web[2].

4 OBSERVATIONAL FEATURES OF SIMULATED STAR CLUSTERS

With NBODY6++GPU simulations done in Section 2, and the computation of GalevNB, we are able to investigate early evolution of the CMD and SED for a stellar population in a real dynamical environment. The output of NBODY6++GPU simulations contains integers to represent information on the stellar type (Hurley et al. 2000) of each individual star (Table 3). This allows one to identify exotic objects in the star cluster based on the evolution of the CMD and SED. It is true that cluster dynamics, such as close stellar encounters or the formation of binaries, can significantly alter the stellar populations in dense stellar systems (Djorgovski & Piotto 1993). Nevertheless, to simplify the NBODY6++GPU simulations that GalevNB works on, we do not consider primordial binaries in the current simulations. Therefore, stellar types 19–22 (binaries) are not present in our simulations. Due to the faintness of a stellar remnant, stellar types 13–15 (though appearing in our examples) are not included in the studies of the CMD and SED.

4.1 SED & CMD Evolution

After integrating fluxes of individual stars, GalevNB outputs the total SED of the star cluster. In the main program, GalevNB.f90, the user can choose to output the SED of certain stellar types. Therefore, specific stars' contribution to the total SED of the cluster can be quantified.

In Figures 1, 3, 5 and 7, we display SEDs of the cluster (black line), of asymptotic giant branch (AGB) stars (red line), of naked helium stars (green line), of white dwarfs (blue), and of core helium burning stars (cyan line) at different ages. Movies of the evolution of the associated SED and CMD are available in the web link provided by footnote 2 in Section 3.2.

At a very early age, massive stars first exhaust their hydrogen in the core and ignite core helium burning. These core helium burning stars are UV-bright (Fig. 1) and very blue (Fig. 2), which are also termed blue loop stars (Stothers & Chin 1991; El Eid 1995). The UV peak in the SED of the cluster (< 1000 Å) is mainly due to the presence of these stars (Fig. 1).

As the cluster evolves, the intensity of the UV-excess drops (Figs. 3, 5 and 7). Besides core helium burning stars, we find another three stellar types producing UV radiation: second AGB stars, white dwarfs and naked helium stars.

(1) Early AGB stars (stellar type $= 5$) are very red, and therefore mainly produce radiation detectable in the red filters (Girardi 2000; Marigo et al. 2008,

[1] *http://silkroad.bao.ac.cn/repos/galevnb*

[2] *http://silkroad.bao.ac.cn/˜xiaoying/*

Table 1 Functions Incorporated in Subroutines Converting Theoretical Parameters into Observational Magnitudes and Spectra

Subroutine	Function
`specint_initialize`	initialize the stellar spectra
`reset_weights`	reset the weight of stellar spectra
`add_star`	integrate the flux of all stars in the cluster
`spec_output`	output spectra
`startomaginit`	initialize the stellar magnitude
`spec2mag`	convolve the stellar spectra with the filter response function
`startomag`	compute magnitudes for stars

Table 2 Contents of the Filter Information File: `filterlist.dat`

Column	Content	ID of zero point
1	Filter name	
2	Corresponding path of the filter response function	
3	ID of selected zero point (default value is 1)	
4	Standard zero point in the Vega magnitude system	1
5	Standard zero point in the AB magnitude system	2
6	Standard zero point in the ST magnitude system	3
7	Optional user-defined zero point	4

Table 3 Stellar Type Defined in the `NBODY6++GPU` Codes

Integer	Stellar type
0	Main sequence (MS) stars with mass$\leq$ $0.7\,M_\odot$
1	MS with mass$\geq$ $0.7\,M_\odot$
2	Hertzsprung Gap
3	Red Giant
4	Core Helium Burning
5	First (early) Asymptotic Giant Branch
6	Second Asymptotic Giant Branch
7	Naked Helium Star MS
8	Naked Helium Star Hertzsprung Gap
9	Naked Helium Star Giant Branch
10	Helium White Dwarf
11	Carbon/Oxygen White Dwarf
12	Oxygen/Neon White Dwarf
13	Neutron Star
14	Black Hole
15	Massless supernova remnant
19	Circularizing binary (c.m. value)
20	Circularized binary
21	First Roche stage (inactive)
22	Second Roche stage

Salaris et al. 2014). After the third dredge-up, helium shells repeatedly flash many times. At this stage, the early AGB stage becomes a thermally pulsing AGB (TPAGB; Marigo et al. 2008; Hurley et al. 2000). The radii of the TPAGB grow so large that mass-loss is significant. At this time, the TPAGB stars reach very high temperature ($> 10^4$ K) and begin to be luminous in the UV filters (Fig. 3). Mass loss will eventually remove all the envelopes of the TPAGB stars, which may be seen as planetary nebulae (see the CMD in Fig. 4). In the NBODY6++GPU code, the phase from TPAGB stars to planetary nebulae is called "second AGB" (stellar type $= 6$).

(2) White dwarfs are born after the TPAGB cases turn into planetary nebulae. Though white dwarfs cool down eventually (Mestel 1952; Liebert 1980; Hansen & Liebert 2003), young white dwarfs are very hot and blue (Mestel 1952; Rauch et al. 2014; Torres et al. 2014), and generate radiation largely in UV ($< 2000\,$Å, Figs. 5 and 7). Even though their luminosity in UV is not high, their contribution to the UV-excess of the cluster is long-term and might not be negligible, since stars continually evolve to white dwarfs.

(3) One short term radiator in UV is a naked helium star, with an extremely blue color in the region that the main-sequence turn-off occurs (Figs. 7 and 8). They are massive stars losing hydrogen envelopes, the so-called Wolf-Rayet stars that are identified in observations (Crowther 2007; Shara et al. 2013). Since naked helium stars only appear at a young age for a short

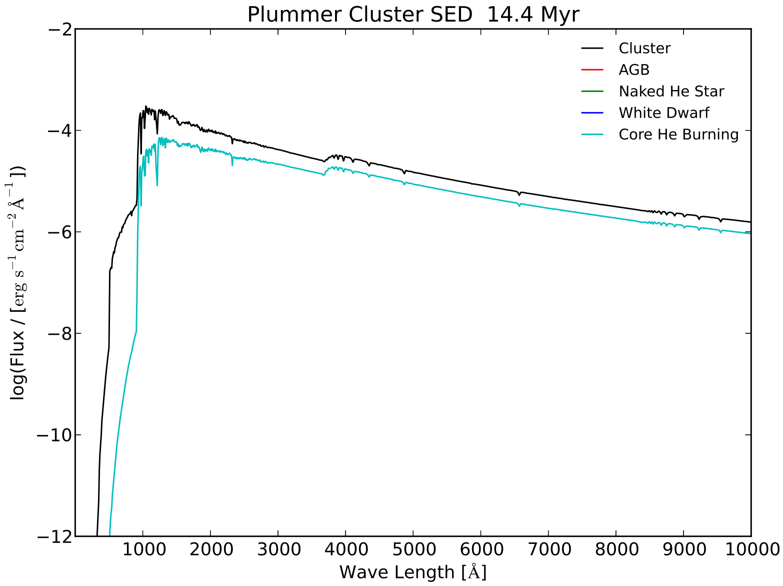

Fig. 1 SED of the simulated cluster (*black line*) and core helium burning stars (*cyan line*) at the age of 14.4 Myr. The SEDs of other stellar types will be shown in the following figures. In this following figures, the SED of core helium burning stars (stellar type $= 4$) is indicated as a cyan line, AGB stars (stellar type $= 5$ and 6) as a red line, naked helium stars (stellar type $= 7, 8, 9$) as a green line, and white dwarfs (stellar type $= 10, 11, 12$) as a blue line.

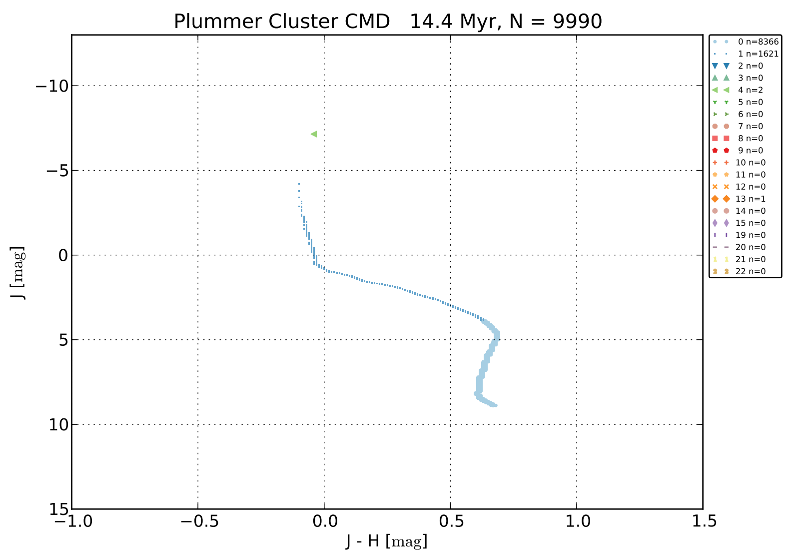

Fig. 2 $J - H$ Color-Magnitude diagram of the simulated cluster at the age of 14.4 Myr. N is the total number of stars, and n is the number of stars of each stellar type indicated in the separate box to the right. Stellar types (see Table 3) are marked with different colors and by different symbols. Main sequence stars (light blue filled round dot: stellar type $= 0$; sky blue one-pixel point: stellar type $= 1$) and core helium burning stars (light green left-pointing-triangle: stellar type $= 4$) appear in this CMD.

time-scale, they cannot influence the UV-excess of the cluster in the long run.

5 DISCUSSION

We present an integrated software solution, `GalevNB`, a translator that bridges `NBODY (6++ / 6)` simulations (with or without GPU acceleration) and observations. We run a short-term dynamical model of a star cluster based on the `NBODY6++GPU` code, producing data for `GalevNB`. `GalevNB` computes observational magnitudes and spectra of stars by theoretical parameters, stellar mass, temperature, luminosity and metallicity, which are generated by `NBODY6++GPU` simulations. In the SED evolution of the simulated cluster, we found a UV-excess in wavelengths shorter than 2000 Å.

A similar phenomenon is found in elliptical galaxies and early-type spiral bulges whose SEDs surpris-

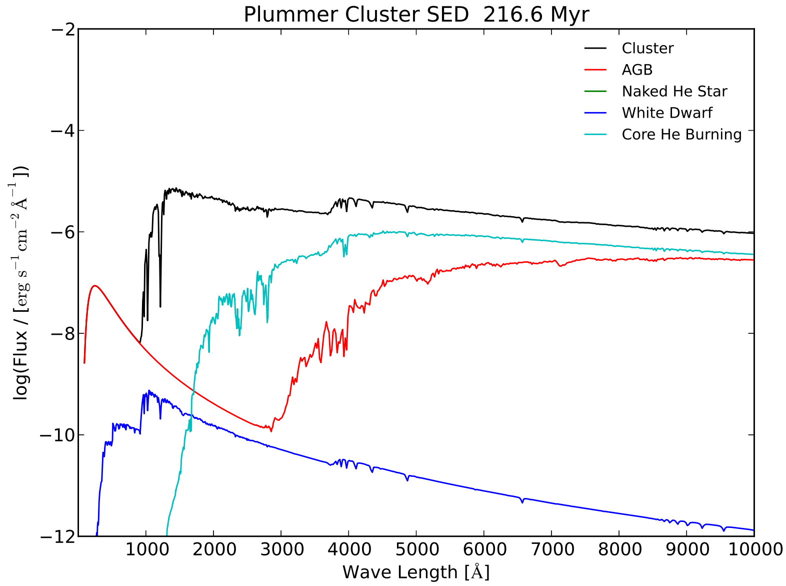

Fig. 3 SED of the simulated cluster (*black line*), AGB stars (*red line*), core helium burning stars (*cyan line*) and white dwarfs (*blue line*) at the age of 216.6 Myr. Color coding is the same as in Fig. 1.

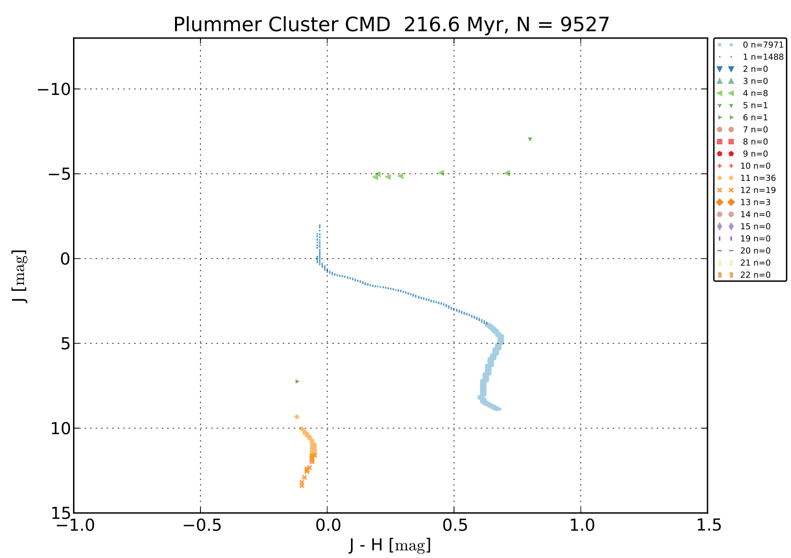

Fig. 4 $J-H$ Color-Magnitude diagram of the simulated cluster at the age of 216.6 Myr. N is the total number of stars, and n is the number of stars of each stellar type indicated in the separate box to the right. Stellar types (see Table 3) are marked with different colors and by different symbols. Main sequence stars (light blue filled round dot: stellar type $=0$; sky blue one-pixel point: stellar type $=1$), core helium burning stars (light green left-pointing-triangle: stellar type $=4$), AGB stars (green downward-triple-point: stellar type $=5$; green upward-triple-point: stellar type $=6$) and white dwarfs (yellow star: stellar type $=11$; orange x-cross: stellar type $=12$) appear in this CMD.

ingly increase to shorter wavelengths over the range 2000 to 1200 Å, (Code 1969; Code et al. 1972; Faber 1983; Burstein et al. 1988; Kurucz 1991), contrary to the expectation of old stellar systems that are usually assumed to be dark in FUV. This rise in the spectrum at wavelengths shorter than 2000 Å is called "UV upturn" or "UV-excess." UV-excess resembles the Rayleigh-Jeans tail of a thermal source with effective temperature larger than 20 000 K (Hills 1971). During recent decades, many efforts have been made to find the "culprits" that lead to UV-excess. In contrast to our simulated cluster whose age is young (up to 655.6 Myr), in most early-type galaxies young massive stars are absent (O'Connell et al. 1986; Welch 1982; Buzzoni et al. 2012). Therefore, old, hot, low-mass stars have become a more popular choice. Extreme blue horizontal branch stars, with core helium burning and very thin envelopes, might be promising for explaining this phenomenon. These stars are found in both metal-

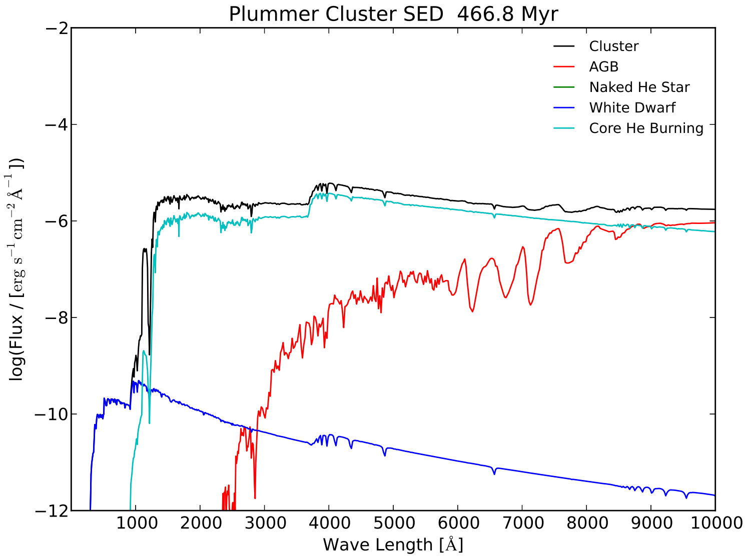

Fig. 5 SED of the simulated cluster (*black line*), AGB stars (*red line*), core helium burning stars (*cyan line*) and white dwarfs (*blue line*) at the age of 466.8 Myr. Color coding is the same as in Fig. 1.

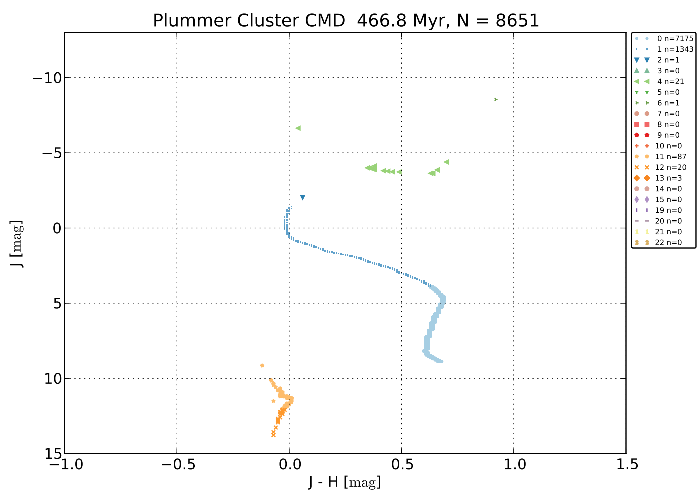

Fig. 6 $J - H$ Color-Magnitude diagram of the simulated cluster at the age of 466.8 Myr. N is the total number of stars, and n is the number of stars of each stellar type indicated in the separate box to the right. Stellar types (see Table 3) are marked with different colors and by different symbols. Main sequence stars (light blue filled round dot: stellar type $= 0$; sky blue one-pixel point: stellar type $= 1$), Hertzsprung gap stars (dark blue filled downward-triangle: stellar type $= 2$), core helium burning stars (light green left-pointing-triangle: stellar type $= 4$), AGB stars (green upward-triple-point: stellar type $= 6$) and white dwarfs (yellow star: stellar type $= 11$; orange x-cross: stellar type $= 12$) appear in this CMD.

rich and metal-poor star clusters (Rich et al. 1997; Ferraro et al. 1998; Li et al. 2013; Buzzoni et al. 2012), which makes their origins somehow ambiguous. Theorists proposed another candidate producing a significant amount of UV radiation, post-AGB stars (Buzzoni & González-Lópezlira 2008), a quarter of which undergo the TPAGB phase (Lawlor & MacDonald 2006). Some studies have suggested that new-born white dwarfs are hot enough to emit a moderate amount of UV photons (Hills 1971; Bica et al. 1996b). Recently, based on detailed computations of binaries, Han et al. (2007) concluded that a brown dwarf binary should be a more promising candidate that can account for the UV-excess.

Most of the candidate stars mentioned above originate in a cluster environment. With the application of `GalevNB` to `NBODY6++GPU` simulation data, we are able to observe the SED evolution of different stellar types. In this way, we discover four kinds of hot, blue stars that are dominant in the UV-excess: core helium burning stars, second AGB stars, white dwarfs and naked helium stars. Among them, second AGB stars are favorable candidates from a theoretical point of view (O'Connell 1999). On the contrary, having a white dwarf as a candidate is controversial (Magris & G. 1993; Landsman et al. 1998) because of its low luminosity. The life time of naked helium stars is very short. Though they are very bright in UV, their short-

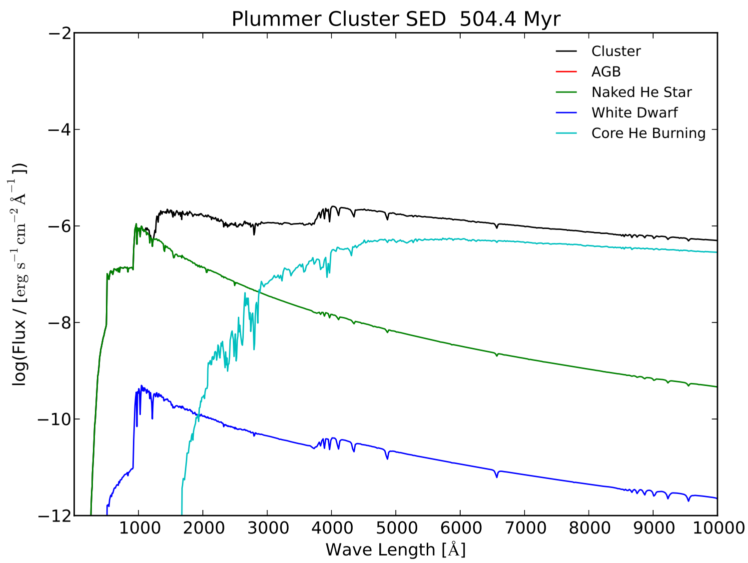

Fig. 7 SED of the simulated cluster (*black line*), naked helium stars (*green line*), core helium burning stars (*cyan line*) and white dwarfs (*blue line*) at the age of 504.4 Myr. Color coding is the same as in Fig. 1.

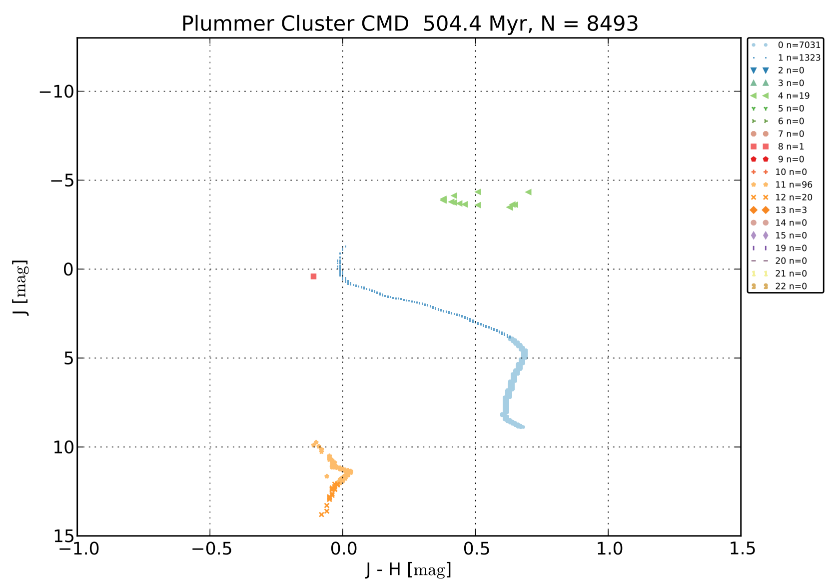

Fig. 8 $J - H$ Color-Magnitude diagram of the simulated cluster at the age of 504.4 Myr. N is the total number of stars, and n is the number of stars of each stellar type indicated in the separate box to the right. Stellar types (see Table 3) are marked with different colors and by different symbols. Main sequence stars (light blue filled round dot: stellar type $= 0$; sky blue one-pixel point: stellar type $= 1$), naked helium burning stars (pink-red square: stellar type $= 8$), core helium burning stars (light green left-pointing-triangle: stellar type $= 4$), and white dwarfs (yellow star: stellar type $= 11$; orange x-cross: stellar type $= 12$) appear in this CMD.

term emission makes them unlikely candidates. However, how the UV radiation from these candidate stars evolves in the long-term is beyond the scope of this paper, which cannot be achieved with a simple stellar model. A detailed `NBODY6++GPU` simulation investigating the evolution of UV-excess in star clusters, with more particles, realistic initial conditions and primordial binaries, will be presented in our forthcoming paper (Pang et al. in prep.). The `NBODY6++GPU` code in its latest GPU accelerated version is publicly available, as described in Wang et al. (2015). We provide our scripts and subroutines of `GalevNB` online[1]. Please note that these are compatible with both versions `NBODY6++ & 6` (with or without GPU acceleration respectively). Users of the other version of `NBODY` may have to adjust some data formats.

For more than a decade "simulating observations of simulations" has been a topic in the community of MODEST (MODelling Dense Star Clusters, see `www.manybody.org/modest/` and Kouwenhoven et al. 2004). Hurley et al. (2005) have published a pioneering study, which presented a full Hertzsprung-Russell diagram (luminosity vs. effective temperature) of all stars in the cluster M67 obtained from a direct N-body simulation with NBODY6, that can be directly compared with observations. These capabilities already come with the standard public versions of NBODY6 and NBODY6++ (with or without GPU acceleration respectively). The Monte Carlo code MOCCA is now also providing similar capabilities (Giersz et al. 2008); recently it has been extended to allow simulated observations of star clusters with specific telescopes that have particular color windows and standard software used by observers (Askar et al. 2015). This work has been driven by future key observational projects (for example those by the HST) for globular clusters (e.g. Milone et al. 2014); however, to fully uncover the 6D dynamical structure and the 3D gravitational potential, as well as the population history of star clusters, pure photometry may not be sufficient. Future deep high resolution spectroscopic and spectrophotometric observations of globular and other star clusters are required in order to uncover one more dimension in velocity (radial velocity) and obtain more information about the stellar populations through analyzing complete spectra. Kacharov et al. (2014) and den Brok et al. (2014) provide examples on how kinematic data provide key insights into the dynamics of globular clusters (rotation and the quest for intermediate mass black holes). For an overview, also see van de Ven (2010). Here the combination of the GALEV codes, previously mainly used for synthesis of galactic stellar populations (Kotulla et al. 2009) with our most recent direct N-body code for star clusters, is a pioneering step to provide the corresponding full spectral information at any time and any region in the cluster, star-by-star or in integrated fields from the models.

Acknowledgements This work is funded by the National Natural Science Foundation of China, Nos. 11443001 (XYP) and 11073025 (RS). XYP extends gratitude to the funds of the National Natural Science Foundation of China, No. 11503015, and of Shanghai education committee, No. 1021ZK 151009027-ZZyy 15104, and of the talents introduction project of the Shanghai Institute of Technology, No. 10120K156031-YJ 2014-05. XYP and RS are members of the Silk Road Project Team based at National Astronomical Observatories, Chinese Academy of Sciences (NAOC, *http://silkroad.bao.ac.cn*), and acknowledge the technical support from this team. CO appreciates funding by the German Research Foundation (DFG) grant OL 350/1-1; CO and RS have been partly supported through computational resources of SFB 881 “The Milky Way System” (subproject Z2) at the University of Heidelberg, Germany, in particular the Milky Way supercomputer hosted and co-funded by the Jülich Supercomputing Center (JSC). XYP appreciates the travel grants of the DFG grant OL 350/1-1.

RS is grateful to support by the Chinese Academy of Sciences Visiting Professorship for Senior International Scientists, Grant Number 2009S1-5, and through the “Qianren” special foreign experts program of China, both at NAOC. The special GPU accelerated supercomputer laohu at the Center of Information and Computing at National Astronomical Observatories, Chinese Academy of Sciences, funded by the Ministry of Finance of the People’s Republic of China under the grant ZDY Z2008-2, has been used for simulations, as well as the smaller GPU clusters titan, hydra and kepler, funded under the grants I/80041-043 and I/84678/84680 of the Volkswagen Foundation at ARI/ZAH, University of Heidelberg, Germany.

RK gratefully acknowledges financial support from the National Science Foundation under Grant No. 1412449, as well as from STScI theory grant HST-AR-12840.01-A.

We appreciate Dr. Peter Anders for promoting and coordinating the collaborations between our N-body team and the GALEV team. Our gratitude also goes to Long Wang and Maxwell Xu Cai for discussion and support in running simulations and programming. We also acknowledge Prof. Richard de Grijs from Peking University and Prof. Zhongmu Li from Dali University for helpful discussion during this work.

References

Aarseth, S. J. 1999, PASP, 111, 1333

Aarseth, S. J. 2003, Gravitational N-Body Simulations (Cambridge: Cambridge Univ. Press)

Ahmad, A., & Cohen, L. 1973, Journal of Computational Physics, 12, 389

Askar, A., Giersz, M., Pych, W., Olech, A., & Hypki, A. 2015, arXiv:1501.00417

Bastian, N., Trancho, G., Konstantopoulos, I. S., & Miller, B. W. 2009, ApJ, 701, 607

Bica, E., Claria, J. J., Dottori, H., Santos, Jr., J. F. C., & Piatti, A. E. 1996a, ApJS, 102, 57

Bica, E., Bonatto, C., Pastoriza, M. G., & Alloin, D. 1996b, A&A, 313, 405

Burstein, D., Bertola, F., Buson, L. M., Faber, S. M., & Lauer, T. R. 1988, ApJ, 328, 440

Buzzoni, A., & González-Lópezlira, R. A. 2008, ApJ, 686, 1007

Buzzoni, A., Bertone, E., Carraro, G., & Buson, L. 2012, ApJ, 749, 35

Cai, M. X., Meiron, Y., Kouwenhoven, M. B. N., Assmann, P., & Spurzem, R. 2015, ApJS, 219, 31

Code, A. D. 1969, PASP, 81, 475

Code, A. D., Welch, G. A., & Page, T. L. 1972, in NASA Special Publication, 310, Scientific Results from the Orbiting Astronomical Observatory (OAO-2), ed. A. D. Code, 559

Crowther, P. A. 2007, ARA&A, 45, 177

den Brok, M., van de Ven, G., van den Bosch, R., & Watkins, L. 2014, MNRAS, 438, 487

Djorgovski, S., & Piotto, G. 1993, in Astronomical Society of the Pacific Conference Series, 50, Structure and Dynamics of Globular Clusters, eds. S. G. Djorgovski, & G. Meylan, 203

El Eid, M. F. 1995, MNRAS, 275, 983
Elson, R. A. W., & Fall, S. M. 1985, ApJ, 299, 211
Faber, S. M. 1983, Highlights of Astronomy, 6, 165
Ferraro, F. R., Paltrinieri, B., Fusi Pecci, F., Rood, R. T., & Dorman, B. 1998, ApJ, 500, 311
Fleck, J.-J., Boily, C. M., Lançon, A., & Deiters, S. 2006, MNRAS, 369, 1392
Giersz, M., Heggie, D. C., & Hurley, J. R. 2008, MNRAS, 388, 429
Giersz, M., & Spurzem, R. 1994, MNRAS, 269, 241
Girardi, L. 2000, in Astronomical Society of the Pacific Conference Series, 211, Massive Stellar Clusters, eds. A. Lançon, & C. M. Boily, 133
Girardi, L., Chiosi, C., Bertelli, G., & Bressan, A. 1995, A&A, 298, 87
Han, Z., Podsiadlowski, P., & Lynas-Gray, A. E. 2007, MNRAS, 380, 1098
Hansen, B. M. S., & Liebert, J. 2003, ARA&A, 41, 465
Hills, J. G. 1971, A&A, 12, 1
Hurley, J. R., Pols, O. R., Aarseth, S. J., & Tout, C. A. 2005, MNRAS, 363, 293
Hurley, J. R., Pols, O. R., & Tout, C. A. 2000, MNRAS, 315, 543
Johnson, L. C., Seth, A. C., Dalcanton, J. J., et al. 2012, ApJ, 752, 95
Kacharov, N., Bianchini, P., Koch, A., et al. 2014, A&A, 567, A69
Kotulla, R., Fritze, U., Weilbacher, P., & Anders, P. 2009, MNRAS, 396, 462
Kouwenhoven, T., Portegies Zwart, S., Gualandris, A., et al. 2004, Astronomische Nachrichten Supplement, 325, 101
Kroupa, P. 2001, MNRAS, 322, 231
Kurucz, R. L. 1991, in Precision Photometry: Astrophysics of the Galaxy, ed. A. G. D. Philip, A. R. Upgren, & K. A. Janes, 27
Kustaanheimo, P. E., & Stiefel, E. 1965, Perturbation Theory of Kepler Motion Based on Spinor Regularization (Astronomical Obervatory)
Landsman, W., Bohlin, R. C., Neff, S. G., et al. 1998, AJ, 116, 789
Larsen, S. S., de Mink, S. E., Eldridge, J. J., et al. 2011, A&A, 532, A147
Lawlor, T. M., & MacDonald, J. 2006, MNRAS, 371, 263
Lejeune, T., Cuisinier, F., & Buser, R. 1997, A&AS, 125, 229
Lejeune, T., Cuisinier, F., & Buser, R. 1998, A&AS, 130, 65
Li, C., de Grijs, R., Deng, L., & Liu, X. 2013, ApJ, 770, L7
Liebert, J. 1980, ARA&A, 18, 363
Magris, C., & G., B. A. 1993, ApJ, 417, 102
Makino, J., & Aarseth, S. J. 1992, PASJ, 44, 141
Marigo, P., Girardi, L., Bressan, A., et al. 2008, A&A, 482, 883
Mestel, L. 1952, MNRAS, 112, 583
Mikkola, S., & Aarseth, S. J. 1993, Celestial Mechanics and Dynamical Astronomy, 57, 439
Miller, R. H. 1966, in IAU Symposium, 25, The Theory of Orbits in the Solar System and in Stellar Systems, ed. G. I. Kontopoulos, 137
Milone, A. P., Marino, A. F., Bedin, L. R., et al. 2014, MNRAS, 439, 1588
Nitadori, K., & Aarseth, S. J. 2012, MNRAS, 424, 545
O'Connell, R. W. 1999, ARA&A, 37, 603
O'Connell, R. W., Thuan, T. X., & Puschell, J. J. 1986, ApJ, 303, L37
Peacock, M. B., Zepf, S. E., & Finzell, T. 2013, ApJ, 769, 126
Peng, E. W., Jordán, A., Côté, P., et al. 2008, ApJ, 681, 197
Peng, E. W., Jordán, A., Blakeslee, J. P., et al. 2009, ApJ, 703, 42
Rauch, T., Werner, K., Quinet, P., & Kruk, J. W. 2014, A&A, 566, A10
Rich, R. M., Sosin, C., Djorgovski, S. G., et al. 1997, ApJ, 484, L25
Salaris, M., Weiss, A., Cassarà, L. P., Piovan, L., & Chiosi, C. 2014, A&A, 565, A9
Sarajedini, A., Barker, M. K., Geisler, D., Harding, P., & Schommer, R. 2007, AJ, 133, 290
Shara, M. M., Bibby, J. L., Zurek, D., et al. 2013, AJ, 146, 162
Spurzem, R. 1999, Journal of Computational and Applied Mathematics, 109, 407
Spurzem, R., & Aarseth, S. J. 1996, MNRAS, 282, 19
Spurzem, R., Berentzen, I., Berczik, P., et al. 2008, in Lecture Notes in Physics, Berlin Springer Verlag, 760, The Cambridge N-Body Lectures, eds. S. J. Aarseth, C. A. Tout, & R. A. Mardling, 377
Stothers, R. B., & Chin, C.-W. 1991, ApJ, 374, 288
Torres, S., García-Berro, E., Krzesinski, J., & Kleinman, S. J. 2014, A&A, 563, A47
Tout, C. A., Aarseth, S. J., Pols, O. R., & Eggleton, P. P. 1997, MNRAS, 291, 732
van de Ven, G. 2010, in IAC Talks, Astronomy and Astrophysics Seminars from the Instituto de Astrofísica de Canarias, 213
Wang, L., Spurzem, R., Aarseth, S., et al. 2015, MNRAS, 450, 4070
Welch, G. A. 1982, ApJ, 259, 77
Whitmore, B. C., Chandar, R., & Fall, S. M. 2007, AJ, 133, 1067